FISEVIER

Contents lists available at SciVerse ScienceDirect

### Materials Science in Semiconductor Processing

journal homepage: www.elsevier.com/locate/mssp



### Review

## Numerical analysis of temporal response of a large exponential-doping transmission-mode GaAs photocathode



Zhipeng Cai a,\*, Wenzheng Yang b, Weidong Tang a, Xun Hou a

- <sup>a</sup> Xi'an Institute of Optics and Precision Mechanics of CAS, State Key Laboratory of Transient Optics and Photonics, 710119 Shaanxi, People's Republic of China
- <sup>b</sup> Xi'an Institute of Optics and Precision Mechanics of CAS, Key Laboratory of Ultrafast Photoelectric Diagnostics Technology, 710119 Shaanxi, People's Republic of China

### ARTICLE INFO

### Available online 27 September 2012

Keywords: Temporal response The average delay time Large exponential-doping GaAs photocathode

### ABSTRACT

The theory of temporal response properties for a large exponential-doping transmission mode GaAs photocathode is discussed in detail. By the introduction of a new concept referred to as "average decay time", the deficiency usually caused by the boundary condition in the previous calculations is effectively eliminated. The analytical results show that the response time of the new GaAs photocathode can be significantly reduced to several picoseconds in the absence of bias. In addition, the thickness of the GaAs absorption layer we obtained is much larger than that of traditional GaAs photocathodes with the same response time, which means that the novel photocathode with ultrafast time response will have higher yield, especially in near-infrared region.

© 2012 Elsevier Ltd. All rights reserved.

### Contents

1.	ntroduction	238
2.	The new structure and the average decay time	239
	2.1. The new structure of the GaAs NEA cathode	239
	2.2. Continuity equation of the photoelectron transport processes	239
	2.3. The average decay time	240
3.	The numerical simulation and discussion	240
	3.1. Simulation analysis of the average decay time based on the results of numerical simulation	241
	3.2. The temporal response analysis for the large exponential-doping NEA photocathode	242
	3.3. The quantum yield	
4.	Conclusions	243
	Acknowledgments	
	References	243

1. Introduction

# \* Correspondence to: Xi'an Institute of Optics and Precision Mechanics of CAS, No. 17 Xinxi Road, New Industrial Park, Xi'an Hi-Tech Industrial Development Zone, Xi'an, 710119 Shaanxi, People's Republic of China. Tel.: +86 158 2975 5614; fax: +86 029 8888 7603.

E-mail address: caizhipeng@opt.ac.cn (Z. Cai).

Thanks to its advantages in high quantum efficiency, narrow electron energy distribution, low emittance and low dark current, GaAs negative electron affinity (NEA) cathodes have found wide applications in photomultipliers (PMT), low-light level image intensifiers, spintronics and electron

beam lithography [1–3]. However, little attention has been paid to its time response properties [4-6]. The temporal response of NEA photocathodes is much slower when compared with multi-alkali photocathodes and Ag-O-Cs photocathodes, which cannot satisfy the requirements in some special fields that need ultra-fast time response, such as high-speed imaging, electron accelerator and electron source of free electron laser (FEL) [7-10]. Guo et al. [11] calculated the temporal response of transmission-mode GaAs photocathodes operated in bias-mode, and their results showed that the response time could be reduced to 10 ps or less. However, the fabrication processes of the fieldassisted photocathodes will deteriorate the response characteristics of GaAs NEA cathodes [12-16]. Zou et al. [17,18] proved that a small gradient-doping mode of absorption layer could improve the characteristics of GaAs NEA cathodes without the need of operation in bias. Therefore, we have designed a large exponential-doping transmissionmode GaAs photocathode to improve the time response feature of GaAs NEA photocathodes to meet the special demands [7–10].

In this paper, a new concept of average decay time is introduced as condition at the emitting boundary to simulate the temporal response processes of the large exponential-doping transmission mode GaAs photocathode. When it is introduced into the simulation, the unphysical sharp peak which appeared in the previous calculation is effectively eliminated. In other words, the photoelectron concentration at the emitting surface of GaAs photocathode is not zero, but a rapidly-decreasing dynamic function varies with time. Based on the improvement, the temporal response processes of the novel photocathode are analyzed by carrier continuity equation with variable coefficients. The analytical results indicate that the new GaAs cathode has ultrafast time response and may break through the limitation of time resolution of traditional GaAs photocathodes.

### 2. The new structure and the average decay time

In this section, the new structure of the GaAs NEA cathode is given and the numerical analysis of the temporal transport processes of the photoelectrons is laid out. Futhermore, the concept of the average decay time is introduced and discussed in detail.

### 2.1. The new structure of the GaAs NEA cathode

Fig. 1 shows the schematic diagram of energy band structure of the large exponential-doping transmission-mode GaAs photocathode. The energy band is divided into two parts: the p-GaAs absorption layer L and the thin emission layer d. The doping concentration N(x) of the absorption layer is described as follow:

$$N(x) = N_0 \exp(-\beta x) \tag{1}$$

where  $N(0)=10^{19} \, \mathrm{cm}^{-3}$ ,  $N(L)=10^{15} \, \mathrm{cm}^{-3}$ ,  $\beta=4 \times \ln 10/L$ , and L, d are the widths of p-GaAs absorption layer and width of the emission layer, respectively.

The thin emission layer d is heavily p-doped to guarantee high quantum efficiency and eliminate surface charge limit (SCL) effect [19,20]. The thickness of this thin emission layer

is expressed by depletion approximation [19,21]

$$d \sim \sqrt{\frac{2\varepsilon \left[E_B - \frac{kT}{q} \ln \frac{N_v}{N(L)}\right]}{qN_A}} \tag{2}$$

where  $N_A$  is the doping concentration of the emission layer, q is electron charge,  $\varepsilon$  is dielectric constant of GaAs,  $E_B$  is band bending of the traditional GaAs photocathodes after Cs:  $O_2$  activation [21],  $N_\nu$  is the effective density of states in the valence band, k is Boltzmann constant, and T=300 K.  $E_{Aeff}$  in Fig. 1 is the effective value of the NEA. Then, the built-in electric field in p-GaAs absorption layer is obtained approximately [19]

$$E = -\frac{dV}{dx} = -\frac{kT}{a}\beta\tag{3}$$

It should be noticed that, the propagation time of light and the effect of incident light on built-in field are ignored in our calculations, considering the electron behaviors are dominant in the temporal response processes of GaAs photocathodes.

### 2.2. Continuity equation of the photoelectron transport processes

Regarding the new structure, the photoelectron transport processes in the emission layer d are ignored considering the fact d e d and then the continuity equation of the photoelectron transport processes for the large exponential-doping GaAs photocathode is expressed as

$$\frac{\partial}{\partial t} \Delta n(x,t) = \frac{\partial}{\partial x} \left[ D_n(x) \frac{\partial}{\partial x} \Delta n(x,t) \right] 
- \frac{\partial}{\partial x} \left[ \mu_n(x) |E| \Delta n(x,t) \right] - \frac{\Delta n(x,t)}{\tau_n(x)}$$
(4)

Einstein relation

$$D_n(x) = \frac{kT}{q} \mu_n(x) \tag{5}$$

The following boundary condition is satisfied [11]

$$D_{n}(x)\frac{\partial}{\partial x}\Delta n(x,t)\bigg|_{x=0} - \mu_{n}(x)|E|\Delta n(x,t)\bigg|_{x=0} = S\Delta n(x,t)\bigg|_{x=0}$$
(6)

$$\Delta n(L,t) = 0 \tag{7}$$

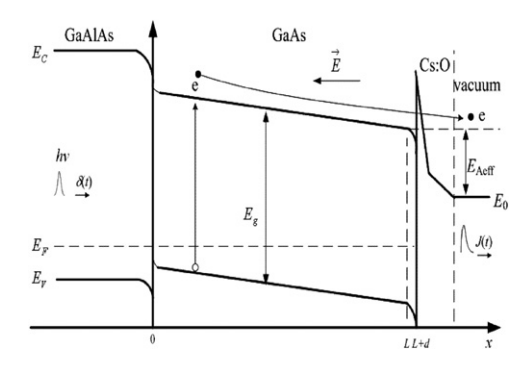


**Fig. 1.** The schematic diagram of energy band of the large exponential-doping photocathode.

where  $\Delta n(x,t)$  denotes the concentration of the photoelectrons,  $D_n(x)$ ,  $\mu_n(x)$ ,  $\tau_n(x)$  [22,23] are the diffusion coefficient of the photo-excited electrons, the photoexcited electron mobility and electron lifetime, respectively. S is the electron recombination velocity at the GaAs/GaAlAs interface. It is noted that the drift velocity  $\mu_n E$  of photoelectrons does not exceed the limitation of the electron velocity v, as mentioned in Ref. [24], and  $\Delta n \ll N(x)$  is considered in calculations.

Under irradiation with an ideal  $\delta$  pulse, initial condition  $\Delta n(x,0)$  can be written as

$$n(x,0) = \alpha I_0(1-R)\exp(-\alpha x) \tag{8}$$

where  $I_0$ ,  $\alpha$ , R are the intensity of incident light, the absorption coefficient of GaAs, the reflection coefficient of GaAs surface, respectively. For transmission-mode GaAs photocathodes, the absorption coefficient  $\alpha$  of GaAs should be in the range of one inverse wavelength.

Once entering the thin emission layer, photoelectrons begin to suffer from severe intervalley scattering in the very strong electric field of the surface depletion region and are emitted to vacuum with a certain probability. Therefore, the flux of emitted photoelectrons is expressed as

$$J(t) = -PD_n(x)\frac{\partial}{\partial x}\Delta n(x,t)\bigg|_{x=L}$$
(9)

where P is surface escape probability.

For the carrier continuity equation with variable coefficients, the analytical solutions for  $\Delta n(x,t)$  cannot be obtained from Eq. (4–8). Therefore, photoelectron continuity equation Eq. (4) is numerically calculated with approximation by the backward difference method, where the numerical solutions are stable without any condition [11].

Using the backward difference method, the thickness of the GaAs layer is divided into M regions, with the step size  $\Delta x$ . The response time region is divided into N regions with equal interval  $\Delta t$ . Then, Eq. (4–8) can be expressed in following discrete forms.

$$a_i n_{i-1}^k + b_i n_i^k + c_i n_{i+1}^k = n_i^{k-1}$$
(10)

$$n(i,0) = F\exp[-\alpha(i-1)dx]$$
 (11)

$$g_1 n_0^k + g_2 n_1^k = 0 (12)$$

$$n_M^k = 0 (13)$$

where,  $i=1,2,...,\ M-1$ ; and  $k=1,2,...,\ N-1,\ \{n_{ik}\}$  is numerical solutions of  $\Delta n(x,t)$ , and

$$\begin{split} F &= \alpha I_0(1-R) \\ a_i &= -D_n(i)\frac{\Delta t}{\Delta x^2} + \frac{D_n(i) - D_n(i-1)}{\Delta x}\frac{\Delta t}{\Delta x} - \mu_n(i)|E|\frac{\Delta t}{\Delta x} \\ b_i &= 1 + 2D_n(i)\frac{\Delta t}{\Delta x^2} - \frac{D_n(i) - D_n(i-1)}{\Delta x}\frac{\Delta t}{\Delta x} + \mu_n|E|\frac{\Delta t}{\Delta x} \\ &+ |E|\frac{u_n(i) - u_n(i-1)}{\Delta x}\Delta t + \frac{\Delta t}{\tau_n(i)} \\ c_i &= -D_n(i)\frac{\Delta t}{\Delta x^2} \\ g_1 &= b_0 - 2\Delta x \frac{S + \mu_n(0)|E|}{D_n(0)} a_0 \\ g_2 &= a_0 + c_0 \end{split}$$

### 2.3. The average decay time

For the non-steady state processes of temporal response, it should be noted that the electron concentration at the emitting boundary is not a constant, that is zero, but a function of time. Therefore, the emitting boundary condition Eq. (13) is unreasonable for the non-steady state processes. Therefore, it is necessary to revise the condition at the emitting boundary under the irradiation with an ideal  $\delta$  pulse light.

Thus, a new concept of "average decay time" is introduced to describe the variation processes of the electron concentration at the emitting boundary. In the proposed method, it is assumed that the electron concentration at the later time was related to that of the former time at the emitting surface. Then, the emitting boundary condition (13) is substituted by Eq. (14)

$$n(M,k) = n(M,k-1)\exp(-\Delta t/\tau')$$
(14)

where  $\tau'$  denotes the average decay time of the electron concentration at the emitting boundary. This parameter is an approximately integrated description for the dynamic variation processes of the surface electron concentration. In this work, it is set to be relevant to the whole photoelectron transport processes of GaAs photocathodes, such as photoelectron generation, electron capture of surface state, e-h pair recombination, and photoelectron emission. Some of them are relevant to thickness and absorption coefficient of GaAs layer. Therefore, the analytical matrix irradiated by  $\delta$  pulse light is expressed as Eq. (15) and the photoelectron transport processes of the new GaAs NEA cathode are obtained.

$$\begin{bmatrix} g_1 & g_1 & & & & & \\ a_1 & b_1 & c_1 & & & 0 & \\ & \vdots & & & & & \\ & a_i & b_i & c_i & & & \\ & & & \vdots & & & \\ & 0 & & a_{M-1} & b_{M-1} & c_{M-1} \\ & & & & 0 & 1 \end{bmatrix} \begin{bmatrix} n_0^k \\ n_1^k \\ \vdots \\ n_i^k \\ \vdots \\ n_{M-1}^k \\ n_{M-1}^k \end{bmatrix}$$

$$= \begin{bmatrix} n_0^{k-1} \\ n_1^{k-1} \\ \vdots \\ n_i^{k-1} \\ \vdots \\ n_{M-1}^{k-1} \\ n_M^{k-1} \exp(-\Delta t/\tau') \end{bmatrix}$$
 (15)

In general, the thickness of GaAs absorption layer should be not less than 0.5  $\mu$ m to avoid imprecision caused by the photoelectron velocity overshoot effect. In addition, the calculations are suitable for the subpicosecond processes when  $L>0.5~\mu$ m, since the electron relaxation time from higher energy states to  $\Gamma$  valleys is in order of subpicosecond [25,26].

### 3. The numerical simulation and discussion

In this section, the theoretical analysis of the average decay time is given. The temporal response behavior of

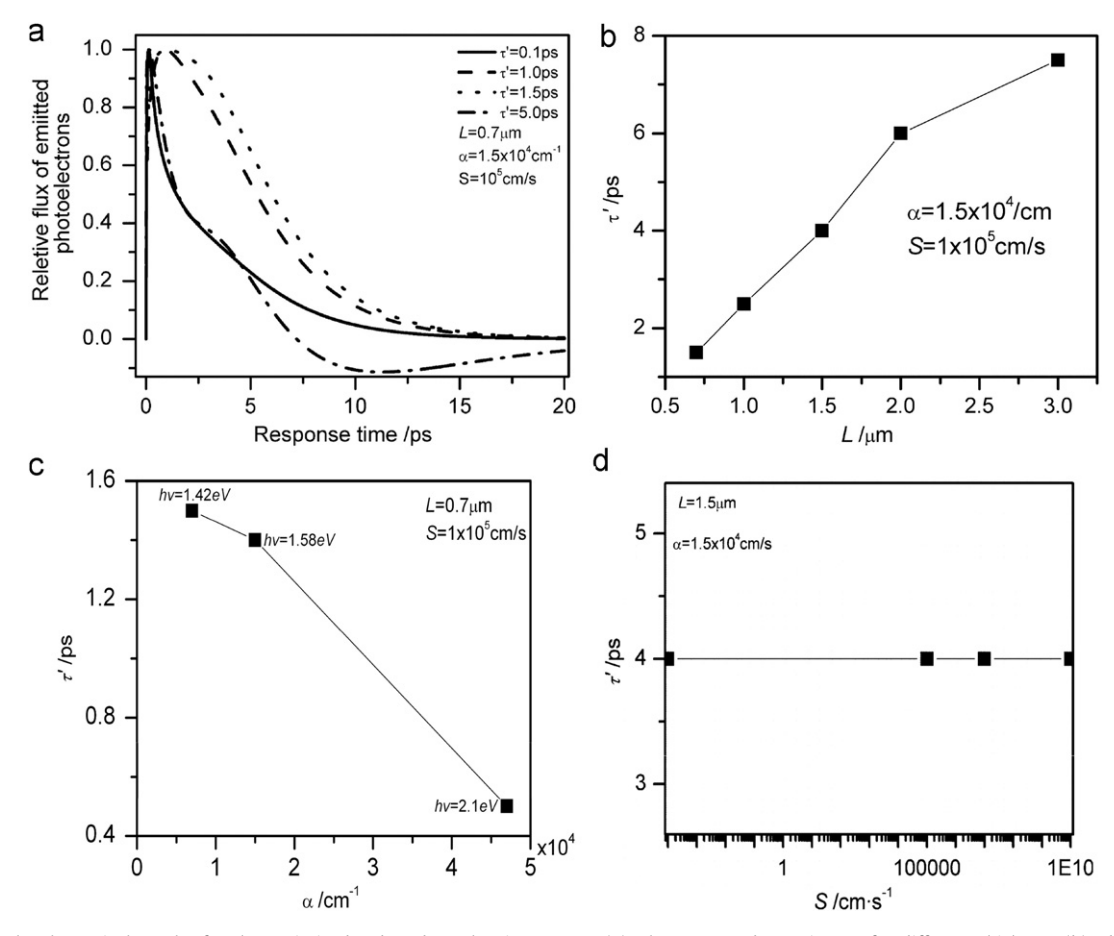


**Fig. 2.** The theoretical results for the optimized  $\tau'$  based on the time curves (a); the average decay time  $\tau'$  for different thickness (b), absorption coefficient (c) and recombination velocity (d) at the GaAs/GaAlAs interface.

GaAs NEA photocathode is analyzed in detail. Meanwhile, the quantum yield of the photocathode is discussed.

## 3.1. Simulation analysis of the average decay time based on the results of numerical simulation

The effects of the thickness of absorption layer and the absorption coefficient on the average decay time are discussed because these parameters are strongly related to the photoelectron transport processes of GaAs NEA cathodes. All the response curves are simulated based on the three parameters, that is, L,  $\alpha$ , S, which denote the thickness of p-GaAs absorption layer, the absorption coefficient of GaAs, the electron recombination velocity at the GaAs/GaAlAs interface, respectively.  $\tau'$  is the average decay time. Photon energy  $E_{hv}$  in Figs. 4–6 corresponds to  $\alpha$ . The values of the different parameters are presented within each figure.

The relationships between L,  $\alpha$ , S and  $\tau'$  are given in Fig. 2. From Fig. 2(a), only when  $\tau'$  is about 1.5 ps, the time response curve is the optimum by comparing the four curves based on the Refs. [7,11,21]. The optimized value of  $\tau'$  is about 1.5 ps under certain condition as shown in Fig. 2(a). That is, Fig. 2(a) shows the optimized  $\tau'$  can be obtained for certain parameters of the novel GaAs

photocathode, since an unsuitable value of  $\tau'$  will lead to unrealistic deformations or negative value of response curves. Based on the method of obtaining optimized  $\tau'$  in Fig. 2(a), each  $\tau'$  is obtained and plotted varying with L,  $\alpha$  and S, as shown in Fig. 2(b)–(d). Fig. 2(b) and (c) shows that thinner GaAs layer and larger absorption coefficient will induce lower valued  $\tau'$ . In contrast, S has almost no or little influence on the  $\tau'$ , as shown in Fig. 2(d) because the GaAs/GaAlAs interface may be far away from the emission surface.

The simulation results indicate that the thickness L of GaAs layer has more important influence on  $\tau$ ' than the other parameters. In addition, we found that the lower limiting value of  $\tau$ ' varies in the range of 0.01–10 ps for the effective thickness L, which could be proved by the simple estimation of  $\tau$ ' obtained from the surface recombination velocity and the narrow band bending region (BBR) [21].

Fig. 3 shows the effect of  $\tau$ ' on the response time curves of the new GaAs photocathode. The curves indicate that the electron concentration at the emitting boundary is a rapid dynamic function of time, which clearly differs from the previous results [11]. In Fig. 3(a), the simulation results show that an unphysical sharp peak always appears under the steady state condition (13) when  $t \rightarrow 0$ . The reason for this

inaccurate results is that J approaches to  $\infty$  at  $t \to 0$  when  $\Delta x$ ,  $\Delta t \to 0$ . As is well known, it is impossible that J approaches to  $\infty$  in limited intensity of light in nature. Therefore, Eq. (13) is not fit for the theoretical simulation of temporal response processes for GaAs photocathodes. While Fig. 3(b) shows that the unreasonable sharp peak at  $t \to 0$  can be effectively eliminated by introducing the average decay time to the condition at the emitting boundary, the revised results are in better agreement with reality than the former results [11]. The simulation results imply that the introduction of the average decay time could better describe various processes of surface photoelectron concentration under  $\delta$  pulse light.

In summary, the average decay time is a parameter describing the dynamic process of the surface electron concentration. The use of it could effectively eliminate the previous defects in calculations. The obtained  $\tau'$  can be used to analyze the temporal response processes of the novel GaAs NEA cathode.

### 3.2. The temporal response analysis for the large exponential-doping NEA photocathode

Fig. 4 shows the time delay of response peak  $(T_m)$  and FWHM  $(\Delta T)$  of the temporal response curves for the GaAs photocathode, respectively. In Fig. 4,  $T_m$  and  $\Delta T$  decrease

with the decreasing of the thickness L of GaAs layer because photoelectron transport path is shortened and the built-in field is increased. Both of  $T_m$  and  $\Delta T$  reach a few picosecond when L approaches to 0.7  $\mu$ m. When  $E_{hv}=1.5$  eV and the thickness L of GaAs layer is 0.7, 1.0, 1.5, 2, 3  $\mu$ m,  $T_m$  is 2.5, 3.5, 8, 21, 58 ps and  $\Delta T$  is 6.5, 12, 28, 52, 120 ps, respectively. When  $E_{hv}=2.1$  eV and L reaches 0.7, 1.0, 1.5, 2, 3  $\mu$ m,  $T_m$  is 3.5, 7.5, 19, 35, 85 ps and  $\Delta T$  is 7, 13, 27, 46, 100 ps, respectively.

From Fig. 4,  $\Delta T$  of the response time can reach 7 ps in the whole absorption region when the thickness of GaAs layer is 0.7  $\mu$ m, which could meet the demand of the electron source of FEL [9]. The above analytical results show that the large exponential-doping method can significantly improve temporal response properties of NEA photocathodes, which indicates that the novel NEA cathode has promising applications in the high speed photoelectron devices.

The effect of S on the time response is shown in Fig. 5. From the figure, it is seen that the response time decreases with the increasing of S, and  $T_m$  and  $\Delta T$  approach to constants, respectively, when  $S > 10^{10}$  cm/s. This result shows that high S is in favor of the temporal response processes for the transmission-mode GaAs photocathode. While higher S will result in more loss of photoelectrons,

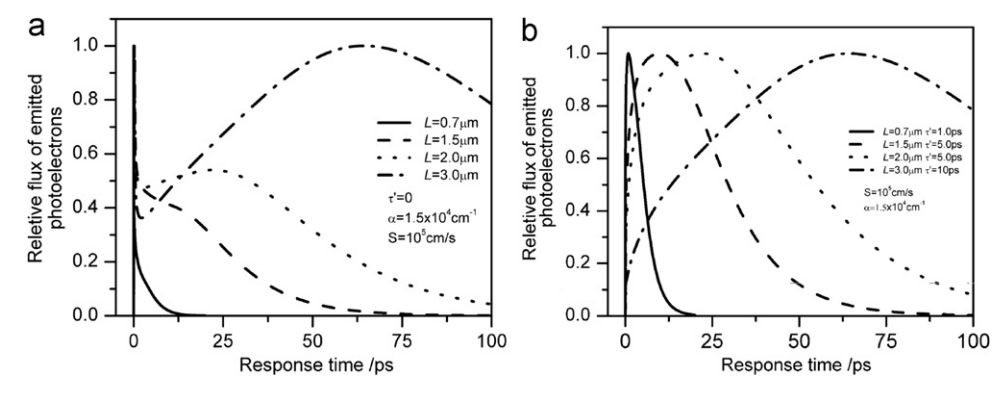
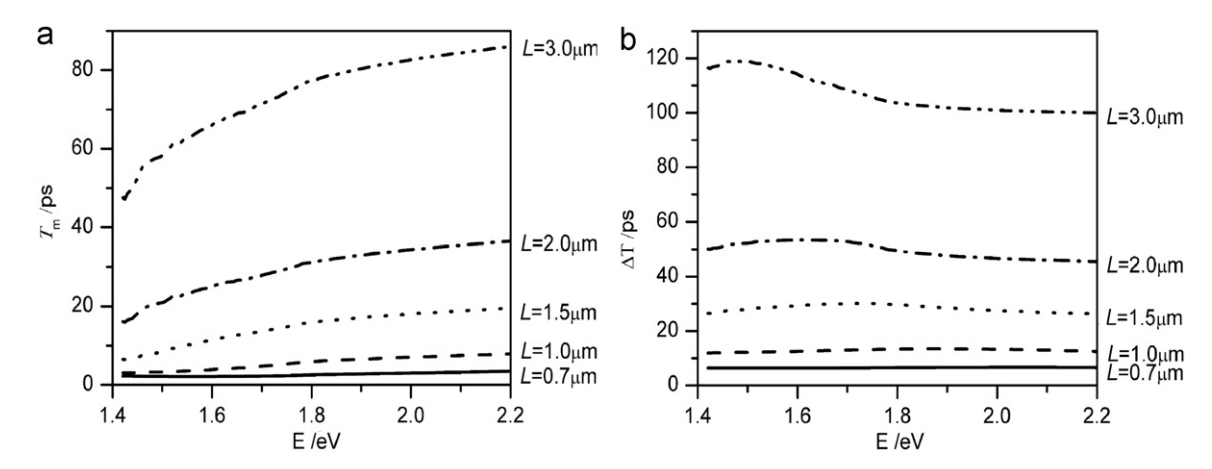


Fig. 3. Normalized response time curves for different L under steady state condition (14) (a) and non-steady state condition (15) (b).



**Fig. 4.** Time response of the GaAs photocathode vs. the energy of photons under  $S=10^5$  cm/s. (a) Maxima  $(T_m)$  of response curves at different L, and (b) FWHM  $(\Delta T)$  of response curves at different L.

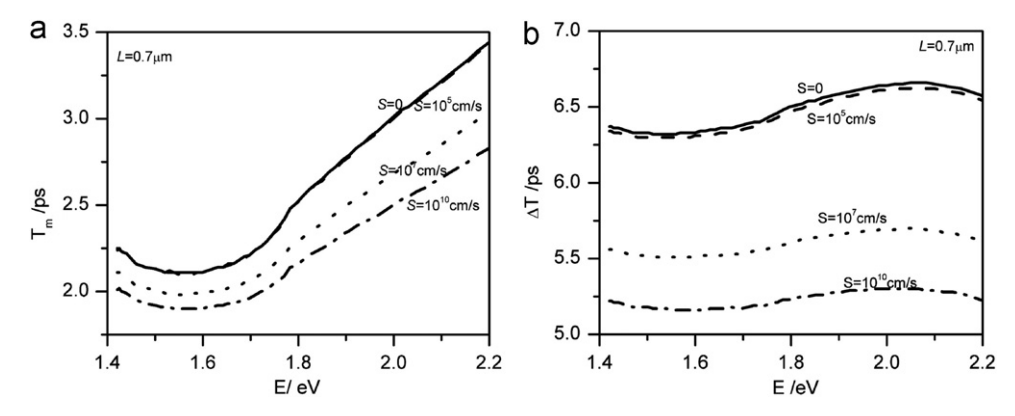
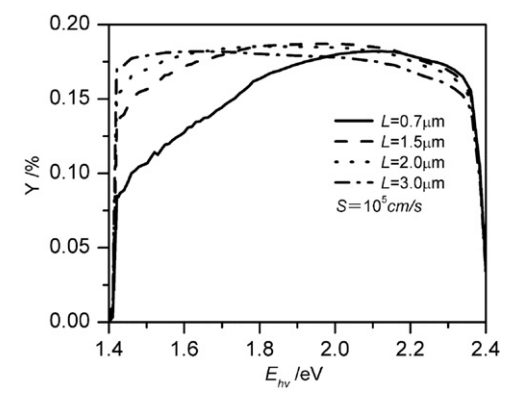


Fig. 5. Time response curves of the GaAs photocathode vs. the energy of photons. (a) Maxima of response curves at different S, and (b) FWHM of response curves at different S.



**Fig. 6.** The quantum yield with the incident photon energy  $E_{hv}$ .

especially under irradiation with the high energy photons. Therefore, the value of *S* should be overall considered in the practical applications.

### 3.3. The quantum yield

The analysis of Section 3.2 shows that the large exponential-doping GaAs photocathode has rapid time response in evidence. However, the surface escape probability of the new GaAs photocathode will be lower than that of traditional GaAs photocathodes because of the lower absolute value  $E_{Aeff}$  of NEA [25], as shown in Fig. 1. The escape probability is about 0.3 by approximate calculations [27–29]. The approximate estimation in Fig. 6 indicates that the quantum yield is about 8–20% in the spectra response region discussed when  $P\sim0.3$ , which is higher than that of traditional GaAs photocathodes in the same response time, especially in near-infrared region. The higher yield is attributed to the thicker GaAs absorption layer. Therefore, the analytical results indicate that the novel GaAs photocathode also has good feature of high yield. [7,9].

#### 4. Conclusions

With the introduction of the average decay time under the condition at the emitting boundary, the problem of the unreasonable peaks appeared in the previous simulations are effectively resolved. Based on this revision and the carrier continuity equation of variable coefficients, the temporal response processes of the large exponential-doping transmission-mode GaAs photocathode have been theoretically discussed. The analytical results demonstrate that the response speed of the new GaAs NEA photocathode is significantly improved. The response time can be reduced to as fast as 7 ps when the thickness of GaAs absorption layer is around 0.7  $\mu m$ . The result suggests that the new GaAs NEA cathode can break through the limitation of time resolution of traditional GaAs photocathodes and is more promising in further potential applications.

### Acknowledgments

This work was financially supported by the Chinese Academy of Sciences.

### References

- [1] J.P. Estrera, E.J. Bende, A. Giordana, J.W. Glesener, M. Iosue, P.P. Lin, T.W. Sinor, Proceedings of SPIE 4128 (2000) 46–53.
- [2] Z. Liu, F. Machuca, P. Pianetta, W.E. Spicer, R.F.W. Pease, Applied Physics Letters 85 (2004) 1541–1543.
- [3] I. Zuic, J. Fabian, S.D. Sarma, Reviews of Modern Physics 76 (2004) 323–410.
- [4] I.V. Bazarov, D.G. Ouzounov, B.M. Dunham, S.A. Belomestnykh, Y.L. Li, X.H. Liu, R.E. Meller, J. Sikora, C.K. Sinclair, Physical Review Special Topics–Accelerators and Beams 11 (2008) 040702–040706.
- [5] I.V. Bazarov, B.M. Dunham, Yulin Li, X.H. Liu, D.G. Ouzounov, C.K. Sinclair, F. Hannon, T. Miyajima, Journal of Applied Physics 103 (2008) 054901–054908.
- [6] A.V. Aleksandrov, M.S. Avilov, R. Calabrese, G. Ciullo, N.S. Dikansky, V. Guidi, G. Lamanna, P. Lenisa, P.V. Logachov, A.V. Novokhatsky, L. Tecchio, B. Yang, Physics Review E 51 (1995) 1449–1452.
- [7] C.C. Phillips, A.E. Hughes, W. Sibbert, Journal of Physics D: Applied Physics 17 (1984) 1713–1725.
- [8] F. Richard, J.R. Schneider, D. Trines, A. Wagner, DESY Report No. 2001-011, Deutsches Elektronen S ynchrotron (DESY), Hamburg.
- [9] L.B. Jones, S.A. Rozhkov, V.V. Bakin, S.N. Kosolobov, B.L. Militsyn, H.E. Scheibler, S.L. Smith, A.S. Tereldiov, 18th International Spin Physics Symposium Spin Physics 1149 (2009) 1057–1064.
- [10] P. Hartmann, J. Bermuch, D.V. Harrach, J. Hoffnann, S. Köbis, E. Reichert, K. Aulenbacher, J. Schuler, M.A. Steigerwald, Journal of Applied Physics 86 (1999) 2245–2249.
- [11] L.H. Guo, J.M. Li, X. Hou, Solid State Electrons 33 (1990) 435-439.

- [12] J.S. Escher, R.L. Bell, P.E. Gregory, S.B. Hyder, T.J. Maloney, G.A. Antypas, IEEE Transactions on Electron Devices ED-27 (1980) 1244–1250
- [13] J.S. Escher, R. Sankaran, Applied Physics Letters 29 (1976) 87-88.
- [14] J.M. Li, L.H. Guo, X. Hou, Journal of Physics D: Applied Physics 22 (1989) 1544–1548.
- [15] L.H. Guo, X. Hou, Journal of Physics D: Applied Physics 22 (1989) 348-353.
- [16] D.G. Fisher, R.E. Enstrom, J.S. Escher, B.F. Williams, Journal of Applied Physics 43 (1972) 3815–3823.
- [17] X.F. Wang, Y.P. Zeng, B.Q. Wang, Z.P. Zhu, X.Q. Du, M. Li, B.K. Chang, Applied Surface Science 252 (2006) 4104–4109.
- [18] J.J. Zou, B.K. Chang, Optical Engineering 45 (2006) 054001–054005.
- [19] J.J. Zou, B.K. Chang, Z. Yang, Chinese Physics Society 56 (2007) 2992–2997.
- [20] A. Herrera-Gómez, G. Vergara, W.E. Spicer, Journal of Applied Physics 79 (1996) 7318–7323.

- [21] K. Aulenbacher, J. Schuler, D.V. Harrach, E. Reichert, J. Röthgen, A. Subashev, V. Tioukine, Y. Yashin, Journal of Applied Physics 92 (2002) 7536–7543.
- [22] S. Tiwar, S.L. Wright, Applied Physics Letters 56 (1990) 563–565.
- [23] A. Sadao, Handbook on Physical Properties of Semiconductors: III-V Compound Semiconductors, vol. 2, Springer, 2004, p. 437.
- [24] K.R. Freeman, G.S. Hobson, IEEE Transactions on Electron Devices ED-19 (1972) 62–70.
- [25] W. Lin, L. Fujimoto, E. Ippen, Applied Physics Letters 50 (1987) 124–126.
- [26] L.H. Guo, X. Hou, Acta Electron Sinica 17 (1989) 118-120.
- [27] J.S. Escher, H. Schade, Journal of Applied Physics 44 (1973) 5309–5313.
- [28] G. Vergara, A. Herrera-Gómez, W.E. Spicer, Journal of Applied Physics 80 (1996) 1809–1815.
- [29] D.G. Fisher, R.E. Enstrom, J.S. Escher, B.F. Williams, Journal of Applied Physics 43 (1972) 3815–3823.